Trimethylene Sulfide···$(HCl)_n$ ($n = 1, 2$) Complexes: A Theoretical Study

H. Valdés and J. A. Sordo*

Laboratorio de Química Computacional, Departamento de Química Física y Analítica, Facultad de Química, Universidad de Oviedo, Julián Clavería 8, 33006 Oviedo, Principado de Asturias, Spain

Received: September 20, 2002; In Final Form: November 26, 2002

The potential energy surfaces (PESs) of the trimethylene sulfide···$(HCl)_n$ ($n = 1, 2$) complexes were explored at the MP2 level of theory by using Pople's and Dunning's basis sets including diffuse functions. Two different axial and equatorial dimer hydrogen-bonded complexes were located on the PESs. The computed geometries are in good agreement with the microwave spectroscopic determination of these two structures. MP4SDTQ//MP2 and QCISD(T)//MP2 single-point calculations were carried out on the significative points on the PESs (minima and transition structures). Comparison among supermolecule uncorrected, counterpoise procedure (CP)-corrected, and BSSE-free complete basis set (CBS) interaction energies suggests that the CP algorithm overcorrects the basis set superposition error (BSSE). However, the supermolecule CP-corrected interaction energies agree rather well with the corresponding BSSE-free symmetry adapted perturbation theory (SAPT) values. The energetic analysis shows that the axial conformer is slightly more stable than the equatorial one, in agreement with the experimental findings. The nature of the interactions in the complexes is analyzed using different theoretical tools: Bader's, NEDA's, Fukui's, and SAPT results are presented and discussed. The interconversion between the two conformers takes place through ring puckering motion involving an energetic barrier of 214−266 cm^{-1} (QCISD//MP2 level). This small barrier is consistent with the experimental observation that only the axial conformer is detected when argon is used as a carrier gas. The possibility for a trimer structure to be present in the molecular beam was analyzed from the theoretical viewpoint. Structural and energetic information on the trimethylene sulfide···$(HCl)_2$ complex from ab initio calculations can be helpful to plan further experimental work to detect such a trimer structure.

Introduction

The tetrahydrofuran (THF)···HCl dimer is a weakly bound molecular association exhibiting two equivalent equilibrium conformations, in agreement with the fact that the acceptor molecule (THF) holds two equivalent geometrical dispositions for the HCl monomer to interact with the nonbonding electron pairs at the oxygen atom. Molecular beam Fourier transform microwave spectroscopy experiments in combination with ab initio calculations allowed for the elucidation of the origin of the tunneling splittings detected experimentally in terms of different mechanisms giving rise to the interconversion between the two equivalent conformations.[1] The corresponding geometries agreed with predictions based on the application of Legon−Millen's rules on angular geometries of hydrogen-bonded dimers.[2,3] Recent experimental[4−6] and theoretical[7] studies on hydrogen-bonded complexes where the acceptor molecule has both nonbonding and π-bonding electron pairs showed that it is hard to establish a general rule for predicting the preferred geometry.

In subsequent experimental[8,9] and theoretical[10,11] studies, the analysis of systems where the acceptor molecule has nonequivalent geometrical dispositions to interact with the nonbonded pairs was tackled. In such cases, Legon−Millen's rules do not apply and thus it is most interesting to examine the different factors leading to a given preference. The experimental data suggested that while for tetrahydropyrane (THP)···HCl dimer the axial conformer is the most stable structure,[8] the equatorial preference is observed for the pentamethylene sulfide (PMS)···(HCl) complex.[9] Ab initio calculations[11] showed that the correction for the basis set superposition error (BSSE) is crucial in predicting the equatorial PMS···HCl conformer as slightly more stable than the corresponding axial complex. However, the well-documented belief (see refs 1 and 12−15 and references therein) that the counterpoise procedure (CP)[16] overcorrects the BSSE at the correlated level strongly suggests that the rather small differences between the CP-corrected interaction energies for the equatorial and axial conformers cannot be considered as definitive.

In a recent work,[17] Alonso and co-workers reported the results of a Fourier transform microwave spectroscopic study on the trimethylene sulfide (TMS)···HCl complex. In this case, the HCl monomer can interact with the nonbonding pairs of the sulfur atom in TMS, giving rise to two different complexes. The authors detected the existence of both the axial and equatorial conformers of the TMS···HCl complex. The analysis of the results led them to the conclusion that the axial conformer is the most stable structure. The geometrical disposition of the conformers was rationalized in terms of the qualitative valence-shell electron-pair repulsion (VSEPR) model.[18] On the other hand, among the different mechanisms for the interconversion between the axial and equatorial forms, Alonso and co-workers speculated that the ring puckering pathway should be the one involving a lower barrier.

Given the importance of the above considerations, concerning the first experimental evidence of the implications of a large-amplitude motion in the conformational behavior of a weakly bound complex,[17] as well as the appropriateness of the ab initio methodology as a tool to rationalize the experimental results[1]

* E-mail: jasg@correo.uniovi.es.

10.1021/jp022110t CCC: $25.00
Published on Web 01/11/2003

in this type of systems,[7,10,11] we carried out a theoretical exploration of the potential energy surface (PES) of the TMS···HCl complex. Our objectives are the following: (a) to locate and characterize (geometry and energy) all the structures on the TMS···HCl PES, (b) to use nonempirical methodologies to shed more light on the nature of the interactions leading to the different conformers, (c) to investigate quantitatively the different pathways for the interconversion between the axial and equatorial forms, and (d) to make a theoretical analysis on the hypothetical formation of a trimer association TMS···$(HCl)_2$ which might be helpful in planning further experimental work.

Methods

The PESs of the TMS···$(HCl)_n$ ($n = 1, 2$) systems were explored at the MP2 level of theory, using Pople's 6-31G(d,p) and 6-31++G(d,p) and Dunning's cc-pVDZ, cc-pVTZ, and aug-cc-pVDZ basis sets. As we will show (see below) and in agreement with previous investigations on similar systems,[1,14,15] the geometries obtained at these levels agree rather well with the experimental data. The structures located on the PESs were characterized either as minima or as saddle points by examining the eigenvalues of the Hessian matrix computed for all basis sets but for the cc-pVTZ one.

To improve the energy predictions, MP4SDTQ//MP2 and QCISD(T)//MP2 single-point calculations were performed. Experience shows[19] that QCISD(T) and CCSD(T) provide rather similar results and that the latter method is, in general, a good approximation to the CCSDT level.[20,21] Therefore, the QCISD(T)//MP2 values should represent reasonable energetic estimates.

The BSSE was corrected by means of two different algorithms: (a) Boys−Bernardi's CP method[16] and (b) complete basis set (CBS) extrapolations.[22]

In the CP method, for a dimer system (AB) formed by two interacting monomers, A and B, the BSSE is estimated as[23]

$$\Delta E^{\mathrm{CP}}(\mathrm{AB}) = E_{\mathrm{AB}}^{\alpha\cup\beta}(\mathrm{AB}) - E_{\mathrm{AB}}^{\alpha\cup\beta}(\mathrm{A}) + E_{\mathrm{AB}}^{\alpha}(\mathrm{A}) - E_{\mathrm{A}}^{\alpha}(\mathrm{A}) - E_{\mathrm{AB}}^{\alpha\cup\beta}(\mathrm{B}) + E_{\mathrm{AB}}^{\beta}(\mathrm{B}) - E_{\mathrm{B}}^{\beta}(\mathrm{B}) \quad (1)$$

where $E_X^{\sigma}(Y)$ is the energy of system Y at the geometry X computed with the basis set σ (α, β, and $\alpha \cup b$) represent the basis sets used to compute the systems A, B, and AB, respectively). It should be noticed that in eq 1 the fragment relaxation terms[24,25] have been included.

The CBS extrapolations are based on the important property of Dunning's correlation-consistent basis sets that exhibit monotonic convergence to an apparent complete basis set limit.[22] We used a mixed exponential/Gaussian function of the form[26]

$$E(x) = E_{\mathrm{CBS}} + B\exp[-(x-1)] + C\exp[-(x-1)^2] \quad (2)$$

where $x = 2$ (DZ), 3 (TZ), or 4 (QZ) and B and C are fitting constants.

Although several alternate expressions are available, our previous experience[21] showed that no significant differences arise from the different extrapolation models.

The CBS extrapolations were carried out from MP2/cc-pVXZ and MP2/aug-cc-pVXZ (X = D, T, Q) calculations. These levels have been shown to provide energies that represent a plausible estimate of the experimental values.[27] Since MP2/cc-pVQZ, MP2/aug-cc-pVTZ, and MP2/aug-cc-pVQZ optimizations (involving 493, 399, and 730 basis functions, respectively) are computationally prohibitive, the MP2/cc-pVQZ//MP2/cc-pVTZ and MP2/aug-cc-pVXZ//MP2/aug-cc-pVDZ (X = T, Q) energies were used in the extrapolation.

By definition, the CBS extrapolations are BSSE-free, thus providing us with a procedure to make reliable predictions on the relative stabilities of the TMS···HCl conformers. In the case of the TMS···$(HCl)_2$ trimer structure, the problems associated with the application of the three-body CP algorithm[28] convert the CBS extrapolations into a valuable alternative to estimate BSSE-free stabilization energies.

Geometry optimizations and single-point calculations were carried out by using the Gaussian 98 packages of programs.[29]

The nature of the interactions in the different conformers was analyzed by using Bader's topological analysis of the electron densities,[30] the natural energy decomposition analysis (NEDA),[31] Fukui's analysis[32] for the wave functions of the complex in terms of different configurations (monotransferred, monoexcited, ...) arising from the electronic exchange among the fragments forming the molecular association (the coefficients representing the weight of different configurations were computed by means of mathematical expressions previously derived),[33] and the symmetry adapted perturbation theory (SAPT).[34] These methodologies allow one to characterize the "binding" of the species formed as well as to get a deeper insight into the nature of the diverse contributions to it. Particularly, NEDA provides supermolecule estimates of the electrostatic (ES) and charge transfer (CT) contributions while SAPT uses a double perturbation series to expand the Hamiltonian allowing for the calculation of the interaction energy in terms of physically interpretable perturbative corrections (electrostatic, induction, dispersion, and exchange energies).[35] All this information is useful not only in rationalizing the experimental data but, as we will show below, also in making theoretical predictions which might help to plan further experimental research.

Results and Discussion

Conformer Geometries. Figure 1 depicts the geometries of the axial ($\mathbf{M_{Ax}}$) and equatorial ($\mathbf{M_{Eq}}$) conformers of the TMS···HCl complex. The geometrical parameters, as computed with different basis sets, are collected in Tables 1 and 2, where the experimental values from microwave spectroscopy[17] are also included for comparison purposes.

It is interesting to note that, contrarily to what is observed for van der Waals complexes,[14,15] all basis set predictions agree rather well. Particularly, the role played by diffuse functions in these moderate[36] hydrogen-bonded complexes seems to be much less important. This behavior is consistent with the fact that dispersion attractive forces are expected to become less important for this type of system where electrostatic contributions should dominate.[37,38] Examination of Tables 1 and 2 shows that the agreement between the theoretical geometries and the ones derived from the spectroscopic measurements is excellent, bearing in mind that the latter values are affected by several uncertainties (mainly the statistical deviation from the least-squares fitting and the assumption that the interacting monomers remain unperturbed upon formation of the complex)[17] and the fact that while the experimental parameters are vibrationally averaged values (r_0), the theoretical estimates correspond to the equilibrium structure (r_e).[39]

Conformer Stabilization Energies. Table 3 collects the energy predictions for both the axial and equatorial structures computed at the different levels of theory employed in the present work. The energy difference between the two conformers is rather small at all levels of theory. In general, the axial conformer is the preferred structure in agreement with the experimental fact that when helium is used as the inert gas,

TABLE 1: MP2 Structural Parameters (Distances, Angles, and Rotational Constants) of the Axial Conformer of TMS···HCl (M_{Ax}) as Computed at Different Levels of Theory (see Figure 1 for Notation)[a]

parameter	6-31G(d,p)	6-31++G(d,p)	cc-pVDZ	cc-pVTZ	aug-cc-pVDZ	exp[d]
r(S−C$_\alpha$)	1.842	1.843	1.857	1.845	1.868	1.82(2)
r(C$_\alpha$−C$_\beta$)	1.536	1.538	1.544	1.537	1.547	1.56(3)
r(C$_\alpha$−C$_\alpha$)	2.270	2.276	2.283	2.280	2.297	2.287(5)
r(S···H)	2.368	2.350	2.285	2.203	2.172	2.28(2)
r(S···Cl)	3.641	3.622	3.578	3.493	3.482	3.539(8)
γ[b]	27.2	25.6	26.6	25.0	25.2	24.(2)
φ	94.1	92.2	91.0	90.2	89.6	92.1(10)
ϕ[c]	90.3	87.9	86.9	86.0	85.6	87.0(7)
θ	11.1	12.2	11.2	11.3	10.6	14.1(8)
∠CSC	76.1	76.3	75.8	76.3	75.9	77.7(11)
A	4523.7	4477.1	4419.6	4465.2	4373.3	4457.5910(27)
B	1338.7	1374.7	1414.1	1483.1	1491.0	1437.25677(62)
C	1255.1	1284.5	1315.9	1378.0	1380.8	1341.24209(61)

[a] Distances are given in angstroms, angles in degrees, and the rotational constants A, B, and C in MHz. [b] γ is the ring-puckering angle. [c] ϕ is the angle between the S···Cl line and the line bisecting the C−S−C angle, considering a collinear arrangement of the S····HCl system (see Figure 1). [d] From ref 17.

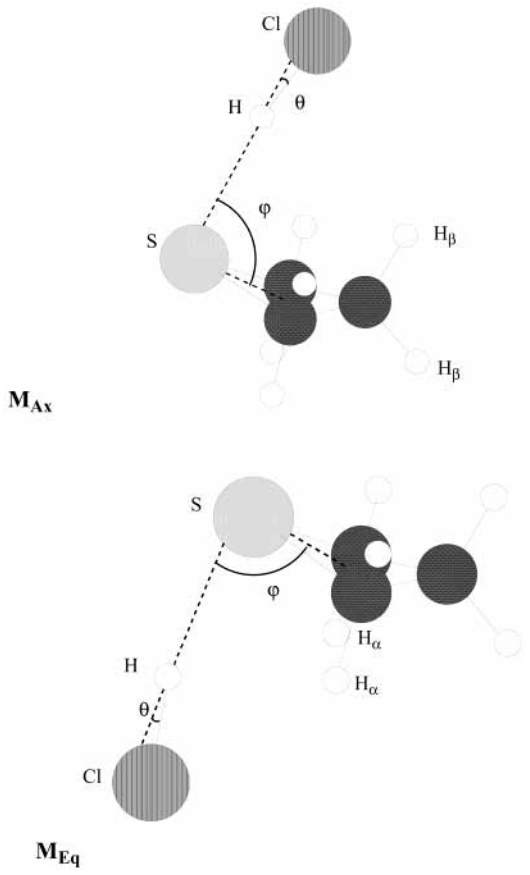

Figure 1. Geometries corresponding to the two TMS···HCl dimer structures located on the MP2 PESs (see Tables 1 and 2 for the values of the geometrical parameters).

only the axial conformer is detected in the microwave spectra.[17] The 6-31++G(d,p) CP-corrected energies break that trend, giving the equatorial conformer as the most stable one by less than 5 cm^{-1}. The approximate nature of the estimate of BSSE by means of the CP algorithm might be the cause of this wrong prediction.

The preference for the axial conformer of TMS···HCl was confirmed by performing CBS MP2 calculations. Table 3 shows that both the cc-pVXZ and aug-cc-pVXZ (X = D, T, Q) extrapolations lead to the conclusion that the axial conformer is the most stable one. Furthermore, the two CBS MP2 values for this conformer (2075 and 2149 cm^{-1}) are rather similar, thus showing that the arguments behind the CBS procedure[22] are founded on solid bases. Interestingly, while the cc-pVXZ series converges to the limit from lower to higher values of the stabilization energies, the aug-cc-pVXZ behavior is the opposite.

It should be stressed that in all cases the MP2 CP-corrected energies are consistently lower than the corresponding MP2 CBS values. Indeed, the MP2/cc-pVXZ (X = D, T, Q) CP values for the axial complex ($\mathbf{M_{Ax}}$) are 1043, 1593, and 1869 cm^{-1}, respectively, while the MP2/cc-pVXZ (X = D, T, Q) CBS value is 2075 cm^{-1}. Similarly, the MP2/aug-cc-pVXZ (X = D, T, Q) CP values for the axial complex are 1684, 1871, and 1985 cm^{-1}, respectively, while the MP2/cc-pVXZ (X = D, T, Q) CBS value is 2149 cm^{-1}. Identical behavior is observed for the equatorial complex (see $\mathbf{M_{Eq}}$ in Table 3).

The above observation agrees with the conclusion by a number of authors that the CP algorithm, when applied at the correlated level, overcorrects the interaction energies (see refs 1 and 12−15 and citations therein for a representative, although nonexhaustive, list of references in this regard).

Nature of the Interactions. Table 4 collects the most representative parameters arising from Bader's, NEDA's, and Fukui's analyses of the supermolecule wave functions of the two conformers of the TMS···HCl complex as computed at the MP2/cc-pVTZ level. Table 5 contains the different contributions to the interaction energies of the axial and equatorial complexes as estimated by perturbation calculations (SAPT). As mentioned elsewhere,[14,15] the calculation of the dispersion contribution requires the use of basis sets including diffuse functions. Therefore, we performed the SAPT calculations using the aug-cc-pVDZ basis set.

Bader's electron density, the Laplacian of the electronic density, and the energy density for both structures are consistent with a shared interaction involving a certain degree of covalency.[40,41] This fact is fully confirmed by NEDA's and Fukui's analyses which show that CT contributions are relevant. Figure 2 depicts the orbitals involved in the most important CT contributions. Besides the HOMO(TMS) → LUMO(HCl) contribution, the HOMO(TMS) → NLUMO(HCl) CT is also important. The NHOMO(TMS) → LUMO(HCl) CT also contributes but to a lesser extent. It is important to stress that the geometry adopted by the two conformers maximizes the overlap between the orbitals intervening in the CT process. This fact reinforces the idea previously suggested,[1] that the Legon−Millen set of rules for predicting geometries of weakly bound complexes (based on pure electrostatic considerations)[3] should be complemented by considering CT contributions, particularly

TABLE 2: MP2 Structural Parameters (Distances, Angles, and Rotational Constants) of the Equatorial Conformer of TMS···HCl (M_{Eq}) as Computed at Different Levels of Theory (see Figure 1 for Notation)[a]

parameter	6-31G(d,p)	6-31++G(d,p)	cc-pVDZ	cc-pVTZ	aug-cc-pVDZ	exp[d]
r(S−C$_\alpha$)	1.842	1.843	1.858	1.845	1.868	1.82
r(C$_\alpha$−C$_\beta$)	1.535	1.537	1.543	1.536	1.546	1.56
r(C$_\alpha$−C$_\alpha$)	2.265	2.270	2.273	2.268	2.287	2.287
r(S···H)	2.336	2.344	2.258	2.189	2.159	2.26(6)
r(S···Cl)	3.582	3.593	3.526	3.455	3.448	3.50(3)
γ[b]	28.4	27.6	29.6	28.6	28.3	24
φ	92.3	91.4	89.0	88.8	88.1	91.1(17)
ϕ[c]	85.7	84.9	82.3	82.2	81.8	84.5(15)
θ	18.6	18.3	18.4	17.9	16.7	18.4(5)
∠**CSC**	75.9	76.0	75.4	75.9	75.5	
A	4876.6	4811.5	4719.1	4770.2	4666.4	4753.9408(19)
B	1286.6	1292.3	1357.1	1408.6	1412.6	1354.88137(77)
C	1231.3	1234.1	1287.3	1335.5	1335.7	1289.97569(73)

[a] Distances are given in angstroms, angles in degrees, and the rotational constants A, B, and C in MHz. [b] γ is the ring-puckering angle. [c] ϕ is the angle between the S···HCl line and the line bisecting the C−S−C angle, considering a collinear arrangement of the S···HCl system (see Figure 1). [d] From ref 17.

TABLE 3: Uncorrected, CP-Corrected (in Parentheses), and CBS Stabilization Energies (D_0, Values Including Zero-Point Energy Corrections,[a] in kcal·mol^{-1}/cm^{-1}) for the Axial (M_{Ax}) and Equatorial (M_{Eq}) Conformers of the TMS···HCl Complex as Computed at Different Levels of Theory

	M_{Ax}			M_{Eq}		
basis	MP2	MP4SDTQ[b]	QCISD(T)[b]	MP2	MP4SDTQ[b]	QCISD(T)[b]
6-31G(d,p)	4.3/1492	3.8/1324	3.7/1301	4.3/1496	3.8/1321	3.7/1295
	(2.7/948)	(2.1/737)	(2.0/711)	(2.6/924)	(2.0/705)	(1.9/677)
6-31++G(d,p)	5.3/1847	4.9/1709	4.8/1690	5.1/1789	4.7/1647	4.7/1626
	(2.7/937)	(2.1/745)	(2.1/730)	(2.7/942)	(2.2/750)	(2.1/733)
cc-pVDZ	5.2/1839	4.5/1590	4.4/1562	5.2/1824	4.5/1564	4.4/1529
	(2.9/1043)	(2.1/750)	(2.0/721)	(3.0/1037)	(2.1/728)	(2.0/689)
cc-pVTZ	5.6/1984			5.6/1944		
	(4.5/1593)			(4.5/1580)		
cc-pVQZ[c]	5.8/2041			5.8/2015		
	(5.3/1869)			(5.3/1852)		
CBS	5.9/2075			5.9/2058		
aug-cc-pVDZ	6.9/2418	6.1/2157	6.0/2103	6.8/2384	6.0/2116	5.8/2057
	(4.8/1684)	(3.9/1368)	(3.7/1318)	(4.7/1671)	(3.8/1343)	(3.6/1288)
aug-cc-pVTZ[d]	6.3/2215			6.3/2215		
	(5.3/1871)			(5.3/1870)		
aug-cc-pVQZ[d]	6.2/2171			6.1/2167		
	(5.6/1985)			(5.6/1984)		
CBS	6.1/2149			6.1/2139		

[a] Zero-point energy contributions were computed from MP2/cc-pVDZ and MP2/aug-cc-pVDZ calculations. [b] MP4SDTQ//MP2 and QCISD(T)//MP2 calculations. [c] MP2/cc-pVQZ//MP2/cc-pVTZ calculations. [d] MP2/aug-cc-pVXZ (X = T, Q)//MP2/aug-cc-pVDZ calculations.

in complexes such as the ones considered in this work for which a shared interaction is present.

Table 5 shows that the electrostatic and induction stabilizing components of the interaction energy are clearly more important than the dispersion contributions, as expected for a hydrogen-bonded interaction. This situation strongly contrasts with what is found in the study of van der Waals complexes where dispersion contributions play a decisive role in the stabilization of the complex.[14,15] Another important point in this context is that for a van der Waals complex the part of the SAPT interaction energy which does not include the correlation energy (E_{int}^{HF} in Table 5) is, in general, repulsive, thus showing that the correlation contribution (mostly through the dispersion component) is required to stabilize the complex. However, in the case of the hydrogen-bonded systems, Table 5 shows that E_{int}^{HF} is already clearly stabilizing.

Alonso and co-workers stressed the remarkable deviation from the collinear arrangement of the S···H−Cl atoms shown by both conformers (see the angle θ in Figure 1 and Tables 1 and 2). These authors speculated that such deviations can be attributed to the existence of secondary hydrogen bonds between the chlorine atom and the nearest hydrogen atom in the methylene groups. Our calculations do support such an interpretation. Indeed, Mulliken population analysis gives $q_{Cl} = -0.3$ au and $q_{H_\alpha,H_\beta} = +0.1$ au (MP2/cc-pVTZ), thus predicting a Cl···H$_\alpha$,H$_\beta$ stabilizing electrostatic interaction (see Figure 1). All the theoretical levels employed yielded the Cl···H$_\beta$ distance in the axial conformer to be slightly shorter than the corresponding Cl···H$_\alpha$ distance in the equatorial complex, in accordance with the experimental results. (The best agreement is found at the MP2/6-31++G(d,p) level where we obtain 3.15 and 3.26 Å for the two distances. The experimental values are 3.20 and 3.26 Å, respectively.)[17] Consistently with the shorter Cl···H$_\beta$ distance, Bader's analysis showed the existence of a bond critical point for the Cl···H$_\beta$ interaction in the axial conformer (see Table 4). The search for the analogue bond critical point for the Cl···H$_\alpha$ interaction in the equatorial conformer was unsuccessful. Interestingly, the axial conformer is the most stable structure.

The importance of the deviation from a S···H−Cl collinear arrangement is demonstrated by the fact that an axial conformer with $\theta = 0$ would become less stable than $\mathbf{M_{Eq}}$ by 20−50 cm^{-1} at the QCISD(T)//MP2 level, depending on the basis set employed.

There are no experimental data available on the dissociation energy of the TMS···HCl axial conformer. Bearing in mind that

TABLE 4: MP2/cc-pVTZ Parameters Arising from Bader's, NEDA's, and Fukui's Analyses of the Wave Functions of the Axial ($\mathbf{M_{Ax}}$) and Equatorial ($\mathbf{M_{Eq}}$) Conformers of the TMS···HCl Complex

	$\mathbf{M_{Ax}}$	$\mathbf{M_{Eq}}$
Bader's Analysis[a]		
S···H bcp(r_c)		
$\rho(r_c)$	0.0327	0.0329
$\nabla^2\rho(r_c)$	0.0437	0.0456
$H(r_c)$	−0.0058	−0.0057
Cl···H$^b_{\alpha\text{ or }\beta}$ bcp(r_c)		
$\rho(r_c)$	0.0061	
$\nabla^2\rho(r_c)$	0.0227	
$H(r_c)$	0.0012	
NEDA Analysis[c]		
ES	−15.9	−16.2
CT	−25.7	−24.1
Fukui's Analysis[d]		
HOMO(TMS) → LUMO(HCl)	0.083	0.083
HOMO(TMS) → NLUMO(HCl)	0.076	0.076
NHOMO(TMS) → LUMO(HCl)	0.037	0.029

[a] Electronic density (ρ), Laplacian of the electronic density ($\nabla^2\rho$), and energy density (H) for the S···H and Cl···H bond critical points are given in au. [b] Closest hydrogens of the methylene groups in the ring. [c] Deformation contributions partly counterbalance the electrostatic (ES) and charge transfer (CT) stabilization contributions (kcal/mol) to yield the final bond energies. [d] Coefficients corresponding to the several terms in ψ(complex) = $C_0\psi$(AB) + $C_1\psi$(A^+B^-) + ... + $C_i\psi$(A^*B) + ... + $C_j\psi$($A^{2+}B^{2-}$) + ... (see ref 36 for further details). Only the most important contributions to ψ, which correspond to charge-transfer configurations, are presented (see Figure 2).

TABLE 5: Different Contributions (See the Text for Definitions) to the SAPT/aug-cc-pVDZ//MP2/aug-cc-pVDZ Interaction Energies [E_{int}(SAPT)] for the Isolated Dimers and for the Dimer Faces of the Trimers (see Figures 1 and 4 for Structural Information)[a]

	isolated dimers		dimers in trimers	
	axial	equatorial	axial	equatorial
$E_{pol}^{(10)}$	−4464	−4160	−3931	−3650
$Er_{pol,}^{(12)}$	−43	8	−39	6
$E_{pol}^{(1)}$	−4507	−4152	−3970	−3644
$Er_{ind,}^{(20)}$	−4589	−4084	−3752	−3267
$^t E_{ind}^{(22)}$	−434	−353	−373	−297
$E_{ind}^{(2)}$	−5023	−4437	−4125	−3564
$E_{disp}^{(20)}$	−2725	−2683	−2452	−2418
$E_{disp}^{(2)}$	−2725	−2683	−2452	−2418
$E_{exch}^{(10)}$	6817	6501	5624	5315
$E_{exch}^{(11)} + E_{exch}^{(12)}$	611	598	540	524
$E_{exch}^{(1)}$	7428	7099	6164	5839
$E_{exch-ind,r}^{(20)}$	3342	2846	2744	2277
$^t E_{exch-ind}^{(22)}$	316	246	273	207
$E_{exch-disp}^{(20)}$	457	416	398	361
$E_{exch}^{(2)}$	4115	3508	3415	2845
E_{int}^{HF}	−558	−543	−658	−635
E_{int}^{CORR}	−1817	−1767	−1654	−1617
E_{int}(SAPT)	−2375	−2269	−2311	−2252
E_{int}^{SUP}(NCP)[b]	−3097	−3010	−3014	−2979
E_{int}^{SUP}(CPR)[b]	−2363	−2347	−2320	−2303

[a] The corresponding MP2/aug-cc-pVDZ interaction energies with [E_{int}^{SUP}(CPR)] and without [E_{int}^{SUP}(NCP)] the CP corrections for the BSSE are also given. All numbers are given in cm^{-1}. [b] To allow comparison with the SAPT values, no ZPE correction and no relaxation energy were included (see in Table 3 the corresponding D_0 values including both ZPE and relaxation energy).

according to Table 3 the QCISD(T)/aug-cc-pVDZ energy is about 1 kcal/mol lower than the MP2/aug-cc-pVDZ value, a reasonable supermolecule prediction for that energy will be 5.1 kcal/mol [obtained by removing 1 kcal/mol from the MP2/aug-cc-pVXZ (X = D, T, Q) CBS value]. Taking into account that the SAPT estimate for the D_0 dissociation energy (after adding both the zero-point energy correction and the relaxation energy to E_{int}(SAPT) in Table 5) is 4.8 kcal/mol, we propose 4.8−5.1 kcal/mol as a plausible range of values for the stabilization energy of the TMS···HCl axial complex.

It is interesting to stress at this point that, in contrast with what has been found in the study of other weakly bound complexes[1,14,15,42] and with the results based on the CBS extrapolations (see previous section), the BSSE-free SAPT interaction energies almost match the CP-corrected values, thus suggesting that no overcorrection exists in the present case.

Dynamics. Let us now comment on the dynamics of the equatorial/axial interconversion process. Figure 3 contains the three saddle point structures located on the PES. $\mathbf{TS_{rp}}$ (C_s symmetry) and $\mathbf{TS_{inv}}$ (C_s symmetry) are first-order saddle points (i.e. transition structures) while **SP** (C_{2v} symmetry) is a second-order saddle point (with two negative eigenvalues in the Hessian matrix). Once more, the geometry predictions for these structures by different basis sets are quite similar.

Graphical analysis of the imaginary frequencies associated with the negative eigenvalues of the Hessian matrix as well as intrinsic reaction coordinate (IRC) calculations,[43,44] as implemented in the Gaussian 98 packages of programs,[29] led to the interconversion paths presented in Scheme 1.

The interconversion between the two conformers $\mathbf{M_{Ax}}$ and $\mathbf{M_{Eq}}$ can take place, in principle, through two different pathways (see Scheme 1): (a) an inversion motion (see $\mathbf{TS_{inv}}$ in Figure 3) in which the HCl unit moves from the equatorial to the axial position and (b) a ring puckering motion (see $\mathbf{TS_{rp}}$ in Figure 3) in which the HCl unit remains basically in the same geometrical disposition. The possibility for an interconversion pathway connecting equivalent conformations ($\mathbf{M_{Ax}} \rightarrow \mathbf{M'_{Ax}}$ or $\mathbf{M_{Eq}} \rightarrow \mathbf{M'_{Eq}}$; crossing lines in Scheme 1) can be discarded as the saddle point involved in such a pathway is a second-order saddle point (see **SP** in Figure 3).

Table 6 shows that the energy barrier associated with $\mathbf{TS_{inv}}$ is too high to allow for a relaxation mechanism converting the less stable conformer ($\mathbf{M_{Eq}}$) into the most stable one ($\mathbf{M_{Ax}}$). Barriers lower than about 400 cm^{-1} are required to make the interconversion affordable.[45] This requirement is fully fulfilled by the $\mathbf{TS_{rp}}$ transition structure. Indeed, Table 6 shows that the energy barrier associated with the ring puckering motion is only 214−266 cm^{-1}, as estimated at the QCISD(T)//MP2 level of theory.

The above theoretical prediction is in full agreement with the experimental observation[17] that when argon is used as a carrier gas, the intensity ratio of about 2.5:1 between axial and equatorial conformers observed with helium does not hold and only the axial form is detected. According to our calculations, the low energy barrier associated with $\mathbf{TS_{rp}}$ (214−266 cm^{-1}) will allow for a full interconversion ($\mathbf{M_{Eq}} \rightarrow \mathbf{M_{Ax}}$) when the heavier, more polarizable, argon inert gas is used as a carrier gas in the microwave spectroscopic experiments.

Possibility of Existence of a Trimer Structure. The impressive advances during this past decade in high-resolution

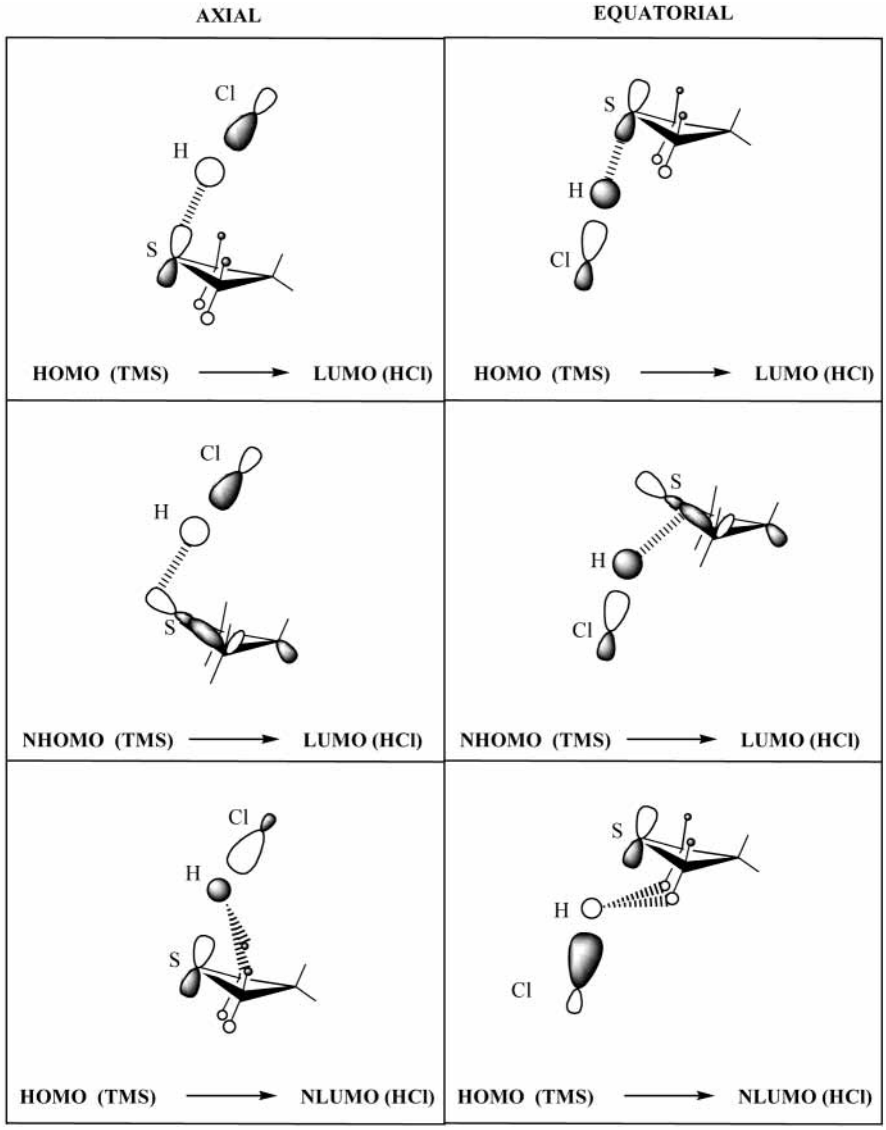

Figure 2. Molecular orbitals of the fragments involved in the most important charge-transfer processes from Fukui's analysis of the wave function of the molecular complexes (see Table 4 for further details).

TABLE 6: Energy Barriers (in kcal·mol^{-1}/cm^{-1}) for the HCl Inversion (TS_{inv}) and Ring Puckering (TS_{rp}) Interconversion Paths between the Axial (M_{Ax}) and Equatorial (M_{Eq}) Conformers of the TMS···HCl van der Waals Complex

	TS_{inv}			TS_{rp}		
basis	MP2	MP4SDTQ	QCISD(T)	MP2	MP4SDTQ	QCISD(T)
6-31G(d,p)	2.7	2.4	2.4	1.0	0.8	0.7
	(935)	(839)	(830)	(340)	(274)	(249)
6-31++G(d,p)	3.4	3.2	3.2	0.9	0.7	0.6
	(1206)	(1135)	(1128)	(301)	(243)	(222)
cc-pVDZ	3.9	3.5	3.5	1.0	0.8	0.8
	(1378)	(1224)	(1209)	(345)	(288)	(266)
cc-pVTZ	4.1			0.7		
	(1437)			(253)		
aug-cc-pVDZ	4.7	4.2	4.2	0.8	0.7	0.6
	(1659)	(1483)	(1458)	(283)	(229)	(214)

spectroscopic techniques using supersonic expansions[46] have given rise to a growing number of publications where weakly bound trimer structures are reported.[47]

In the previous sections we analyzed the two possible dimers ($\mathbf{M_{Ax}}$, $\mathbf{M_{Eq}}$) experimentally detected for the TMS···HCl system. Examination of the geometries for the two complexes in Figure 1 clearly suggests the possibility for a trimer structure [TMS···$(HCl)_2$] to be present in the molecular beam. In such a structure, the two HCl monomer units should occupy the axial and equatorial positions experimentally detected for the two dimer complexes ($\mathbf{M_{Ax}}$, $\mathbf{M_{Eq}}$). On some occasions, a number of unassigned transitions in the microwave spectra of dimer complexes can be associated with the presence of trimer structures in the molecular beam.[48,49] The theoretical structural information provided in this section might be useful in planning further experimental work to detect trimer species in the gas mixtures containing TMS and HCl samples.

Figure 4 shows the theoretically predicted geometry for the TMS···$(HCl)_2$ trimer structure, and Table 7 collects all the geometrical parameters as computed at the different levels of

SCHEME 1

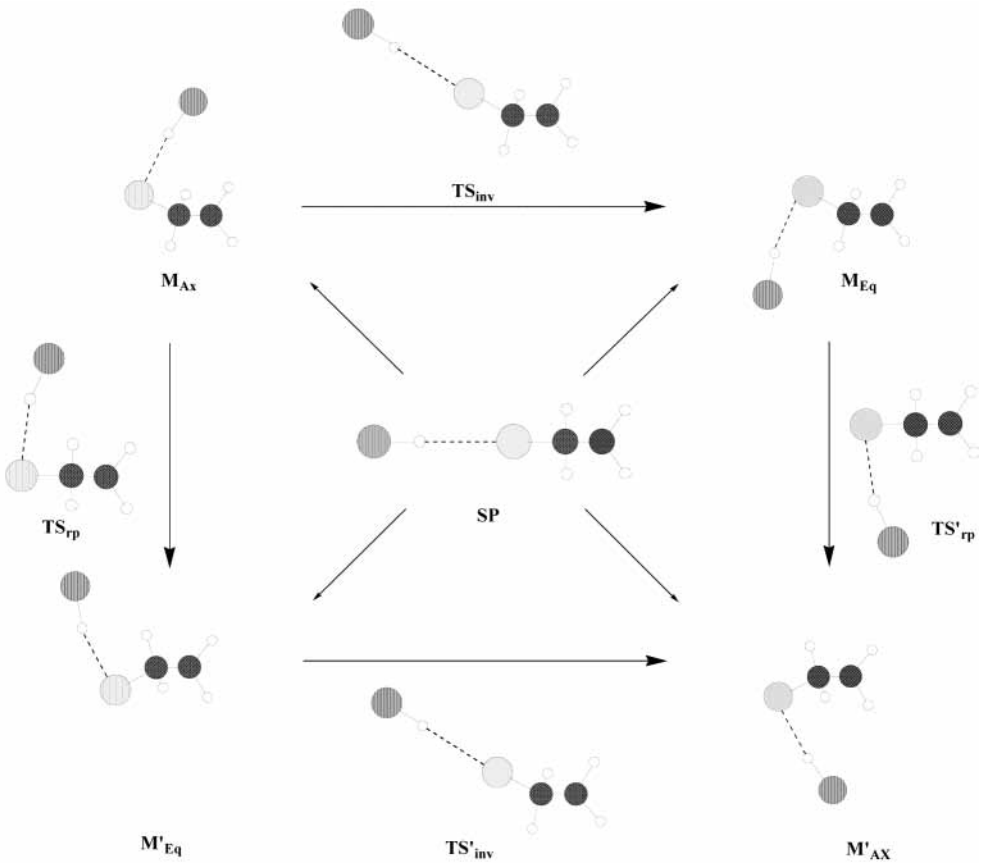

theory employed in this work. As one could expect, bearing in mind the two dimer structures discussed in previous sections, the trimer geometry is basically a superposition of the two dimer geometries $\mathbf{M_{Ax}}$ and $\mathbf{M_{Eq}}$.

Table 5 shows that the losses in stabilizing contributions from the electrostatic, induction, and dispersion components when the TMS···HCl dimers are forming part of the trimer structure are almost totally compensated by a notable reduction in the repulsive exchange contribution. The global effect is that the two TMS···HCl dimer faces in the trimer are only slightly less stable than their corresponding isolated dimer structures. It is interesting to mention that the CP corrected stabilization (De) energy for the axial dimer in the trimer (2163 cm^{-1}) is slightly larger than the corresponding value for the axial isolated dimer (2157 cm^{-1}). Of course, it represents an anomalous result arising from the application of the CP algorithm (Table 5 contains interaction energies computed by subtracting from De the relaxation energy).

Finally, Table 8 collects the stabilization energies for the TMS···$(HCl)_2$ trimer as estimated at the different levels of theory employed in this work. Data in this table clearly support, from a thermodynamical point of view, the viability of the formation of a trimer structure in the molecular beam.

Conclusions

The PESs for the TMS···$(HCl)_n$ (n = 1, 2) complexes were extensively explored at the MP2 level of theory, using Pople's 6-31G(d,p) and 6-31++G(d,p) and Dunning's cc-pVDZ, cc-pVTZ, and aug-cc-pVDZ basis sets. MP4SDTQ//MP2 and QCISD(T)//MP2 single-point calculations were carried out in order to improve the energy predictions.

While the CBS MP2 calculations suggest that the CP algorithm overcorrects the interaction energies as estimated at the correlated level, the BSSE-free SAPT interaction energies almost match the corresponding CP corrected values.

Bearing in mind the goals proposed in the Introduction section of this article, the main conclusions can be summarized as follows:

(a) Two minima structures corresponding to the axial and equatorial conformers of the TMS···HCl dimer and two transition structures representing inversion and ring-puckering motions, respectively, were located on the PES. A third saddle point structure was also located, but it corresponds to a chemically meaningless second-order saddle point.

The MP2 geometries for the two minima agree reasonably well with the two experimentally detected conformers. Most of the theoretical levels employed, and particularly the most sophisticated ones, show the axial conformer to be the most stable structure, in agreement with the experimental evidence. The supermolecule MP2/aug-cc-pVXZ (X = D, T, Q) CBS estimate for the stabilization energy of the axial conformer, once corrected for higher order correlation effects as estimated at the QCISD(T)/aug-cc-pVDZ//MP2/aug-cc-pVDZ level (5.1 kcal/mol), consistently coincides with the perturbation theory (SAPT/aug-cc-pVDZ) prediction (4.8 kcal/mol).

(b) Bader's, NEDA's, Fukui's, and SAPT's analyses helped us to characterize and classify the type of interactions present in the TMS···$(HCl)_n$ (n = 1, 2) complexes. In sharp contrast with what is found in van der Waals weakly bound complexes, the electrostatic and induction contributions in the present hydrogen-bonded structures are much more important than the dispersion component. Furthermore, the conformers are stable structures already at the Hartree−Fock level of theory.

Bader's topological analysis shows the existence of stabilizing secondary hydrogen bonding interactions in the most stable axial conformer.

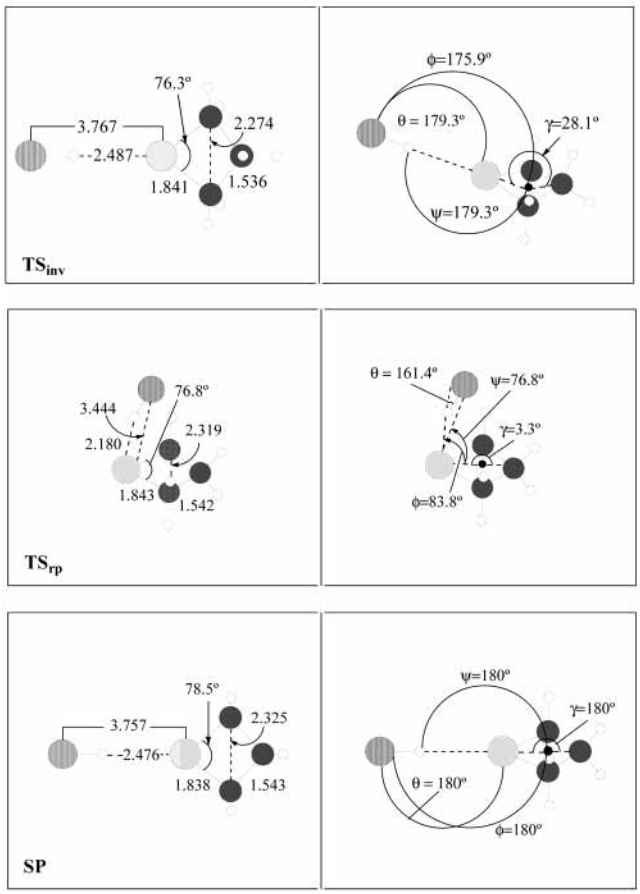

Figure 3. Saddle points located on the MP2 PESs corresponding to the interconversion between the two TMS···HCl dimers. **TS$_{inv}$** and **TS$_{rp}$** are transition structures while **SP** is a second-order saddle point. Distances are in angstroms, and angles are in degrees (see Table 6 for the corresponding energy barriers).

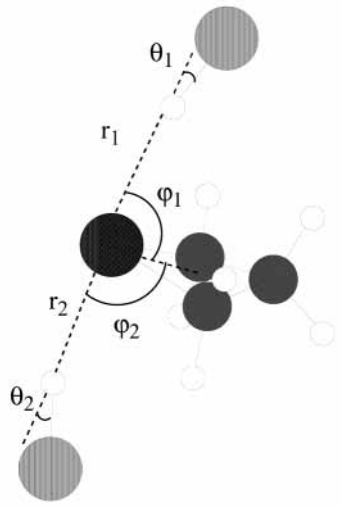

Figure 4. Geometry corresponding to the TMS···$(HCl)_2$ trimer located on the MP2 PES (see Table 7 for the values of the geometrical parameters).

(c) The QCISD(T)/aug-cc-pVDZ energy barriers associated with the inversion motion (**TS$_{inv}$**: 1458 cm^{-1}) and ring-puckering motion (**TS$_{rp}$**: 214 cm^{-1}) suggest that the interconversion between the less stable (equatorial) and the most stable (axial) conformers should take place through a ring-puckering motion. The corresponding barrier is small enough to allow for a full interconversion when a heavy inert gas such as argon is used as a carrier gas in the supersonic jet, in full agreement with experimental observations.

TABLE 7: MP2 Structural Parameters (Distances, Angles, and Rotational Constants) of the TMS···$(HCl)_2$ Trimer as Computed at Different Levels of Theory (see Figure 4 for Notation)[a]

parameter	6-31G(d,p)	6-31++G(d,p)	cc-pVDZ	cc-pVTZ	aug-cc-pVDZ
r(S−C$_\alpha$)	1.844	1.846	1.860	1.848	1.871
r(C$_\alpha$−C$_\beta$)	1.536	1.538	1.544	1.537	1.548
r(C$_\alpha$−C$_\alpha$)	2.269	2.282	2.282	2.282	2.302
r_1(S···H)	2.428	2.397	2.370	2.272	2.246
r_2(S···H)	2.403	2.401	2.349	2.263	2.238
r_1(S···Cl)	3.688	3.654	3.646	3.544	3.537
r_2(S···Cl)	3.623	3.628	3.585	3.503	3.501
γ[b]	27.9	24.0	27.5	24.8	24.0
φ_1	95.4	91.9	92.1	90.7	89.2
φ_2	93.7	91.3	89.8	89.0	87.5
ϕ_1[c]	90.7	86.6	87.0	85.6	84.3
ϕ_2[c]	85.9	83.8	81.7	81.3	80.2
θ_1	13.6	15.2	14.3	14.0	13.3
θ_2	22.4	21.7	22.7	21.3	19.9
∠**CSC**	75.9	76.4	75.7	76.3	75.9
A	3532.6	3799.5	3843.6	3951.4	3942.8
B	507.5	514.3	522.4	550.9	554.5
C	480.2	491.5	499.7	527.6	531.5

[a] Distances are given in angstroms, angles in degrees, and the rotational constants, A, B, and C, in MHz. [b] γ is the ring-puckering angle. [c] ϕ is the angle between the S···Cl line and the line bisecting the C−S−C angle, considering a collinear arrangement of the S···HCl system (see Figure 4).

TABLE 8: Stabilization Energies [D_0 in kcal·mol^{-1} and in cm^{-1} (in parentheses)] for the TMS···$(HCl)_2$ van der Waals Trimer Complex

	D_0		
	MP2	MP4SDTQ	QCISD(T)
6-31G(d,p)	7.7 (2685)	6.9 (2405)	6.7 (2363)
6-31++G(d,p)	9.8 (3416)	9.2 (3194)	9.1 (3156)
cc-pVDZ[a]	9.6 (3349)	8.4 (2933)	8.2 (2877)
cc-pVTZ	10.3 (3602)		
cc-pVQZ[b]	10.6 (3727)		
CBS	10.9 (3803)		
aug-cc-pVDZ	12.2 (4274)	11.0 (3851)	10.7 (3743)

[a] A rather small imaginary frequency (7 cm^{-1}) appeared at this level of theory (ZPE was estimated from the MP2/6-31G(d,p) calculations). [b] MP2/cc-pVQZ//MP2/cc-pVTZ calculations.

(d) The possibility for a TMS···$(HCl)_2$ trimer structure to be present in the molecular beam was also assessed. A geometry consisting of two HCl monomer units occupying similar possitions as those found in the TMS···HCl dimer complexes was located and characterized as a minimum structure. The stabilization energy computed for this trimer (3743 cm^{-1} at the QCISD(T)/aug-cc-pVDZ//MP2/aug-cc-pVDZ level) suggests that it may be present in the molecular beam. The structural information provided in this work might be useful to plan further experimental work in order to detect such a trimer structure.

Acknowledgment. J.A.S. wishes to thank DGU (Servicio de Acciones de Promocion y Movilidad, Madrid, Spain) for a grant that made possible his stay at Rice University, where this article was prepared. The authors thank Prof. S. Fraga (Uni-

versity of Alberta, Canada) for helpful comments. Financial support through project BQU2001-3660-C02-01 is also acknowledged.

References and Notes

(1) Lopez, J. C.; Alonso, J. L.; Lorenzo, F. J.; Rayon, V. M.; Sordo, J. A. *Chem. Phys.* **1999**, *111*, 6363.

(2) Legon, A. C.; Millen, D. J. *Faraday Discuss. Chem. Soc.* **1982**, *73*, 71.

(3) Legon, A. C.; Millen, D. J. *Chem. Soc. Rev.* **1987**, *16*, 467.

(4) Cooke, S. A.; Corlett, G. K.; Legon, A. C. *J. Chem. Soc., Faraday Trans.* **1998**, *94*, 1565.

(5) Cooke, S. A.; Corlett, G. K.; Holloway, J. H.; Legon, A. C. *J. Chem. Soc., Faraday Trans.* **1998**, *94*, 2675.

(6) Cooke, S. A.; Holloway, J. H.; Legon, A. C. *Chem. Phys. Lett.* **1998**, *298*, 151.

(7) Valdes, H.; Rayon, V. M.; Sordo, J. A. *Chem. Phys. Lett.* **1999**, *309*, 265.

(8) Antolinez, S.; Lopez, J. C.; Alonso, J. L. *Angew. Chem., Int. Ed. Engl.* **1999**, *38*, 1772.

(9) Sanz, M. E.; Lopez, J. C.; Alonso, J. L. *Chem. Eur. J.* **1999**, *5*, 3293.

(10) Valdes, H.; Rayon, V. M.; Sordo, J. A. *Chem. Phys. Lett.* **2000**, *320*, 507.

(11) Valdes, H.; Sordo, J. A. *Chem. Phys. Lett.* **2001**, *333*, 169.

(12) Morokuma, K.; Kitaura, K. *Chemical Application of Atomic and Molecular Electronic Potentials*; Politzer, P., Ed.; Plenum: New York, 1981.

(13) Hunt, S. W.; Leoplod, K. R. *J. Phys. Chem. A* **2001**, *105*, 5498.

(14) Valdes, H.; Sordo, J. A. *J. Comput. Chem.* **2002**, *23*, 444.

(15) Valdes, H.; Sordo, J. A. *J. Phys. Chem. A* **2002**, *106*, 3690.

(16) Boys, S. F.; Bernardi, F. *Mol. Phys.* **1970**, *19*, 553.

(17) Sanz, M. E.; Lesarri, A.; Lopez, J. C.; Alonso, J. L. *Angew. Chem., Int. Ed.* **2001**, *40*, 935.

(18) Gillespie, R. J.; Nyholm, R. S. *Q. Rev. Chem. Soc.* **1957**, *11*, 339.

(19) Jensen, F. *Introduction to Computational Chemistry*; Wiley: Chichester, 1999.

(20) Feller, D. A.; Sordo, J. A. *J. Chem. Phys.* **2000**, *112*, 5604.

(21) Feller, D.; Sordo, J. A. *J. Chem. Phys.* **2000**, *113*, 485.

(22) Dunning, T. H., Jr. *J. Phys. Chem. A* **2000**, *104*, 9062.

(23) Emsley, J.; Hoyte, O. P. A.; Overill, R. E. *J. Am. Chem. Soc.* **1978**, *100*, 3303.

(24) Xantheas, S. S. *J. Chem. Phys.* **1996**, *104*, 8821.

(25) Rayon, V. M.; Sordo, J. A. *Theor. Chem. Acc.* **1998**, *99*, 68.

(26) Peterson, K. A.; Woon, D. E.; Dunning, T. H., Jr. *J. Chem. Phys.* **1994**, *100*, 7410.

(27) Feller, D.; Peterson, K. A. *J. Chem. Phys.* **1998**, *108*, 154.

(28) Lendvay, G.; Mayer, I. *Chem. Phys. Lett.* **1998**, *297*, 365.

(29) Frisch, M. J.; Trucks, G. W.; Schlegel, H. B.; Scuseria, G. E.; Robb, M. A.; Cheeseman, J. R.; Zakrzewski, V. G.; Montgomery, J. A., Jr.; Stratmann, R. E.; Burant, J. C.; Dapprich, S.; Millam, J. M.; Daniels, A. D.; Kudin, K. N.; Strain, M. C.; Farkas, O.; Tomasi, J.; Barone, V.; Cossi, M.; Cammi, R.; Mennucci, B.; Pomelli, C.; Adamo, C.; Clifford, S.; Ochterski, J.; Petersson, G. A.; Ayala, P. Y.; Cui, Q.; Morokuma, K.; Malick, D. K.; Rabuck, A. D.; Raghavachari, K.; Foresman, J. B.; Cioslowski, J.; Ortiz, J. V.; Stefanov, B. B.; Liu, G.; Liashenko, A.; Piskorz, P.; Komaromi, I.; Gomperts, R.; Martin, R. L.; Fox, D. J.; Keith, T.; Al-Laham, M. A.; Peng, C. Y.; Nanayakkara, A.; Gonzalez, C.; Challacombe, M.; Gill, P. M. W.; Johnson, B.; Chen, W.; Wong, M. W.; Andres, J. L.; Gonzalez, C.; Head-Gordon, M.; Replogle, E. S.; Pople, J. A. *Gaussian 98*; Gaussian Inc.: Pittsburgh, PA, 1998.

(30) Bader, R. F. W. *Atoms in Molecules. A Quantum Theory*; Oxford University Press: New York, 1990.

(31) Reed, A. E.; Curtiss, L. A.; Weinhold, F. *Chem. Rev.* **1988**, *88*, 899.

(32) Fujimoto, H.; Kato, S.; Yamabe, S.; Fukui, K. *J. Chem. Phys.* **1974**, *60*, 572.

(33) Menendez, M. I.; Sordo, J. A.; Sordo, T. L. *J. Phys. Chem.* **1992**, *96*, 1185.

(34) Bukowski, R.; Jankowski, P.; Jeziorski, B.; Jeziorski, M.; Kucharski, S. A.; Moszynski, R.; Rybak, S.; Szalewicz, K.; Willians, H. L.; Wormer, P. E. S. *SAPT96: An ab initio Program for Many-Body Symmetry-Adapted Perutbation Theory Calculations of Intermolecular Interaction Energies;* University of Delaware and University of Warsaw: 1996.

(35) Jeziorski, B.; Moszynski, R.; Szalewicz, K. *Chem. Rev.* **1994**, *94*, 1887.

(36) Jeffrey, G. A. *An Introduction to Hydrogen Bonding*; Oxford University Press: New York, 1997.

(37) Stone, A. J. *The Theory of Intermolecular Forces*; Clarendom Press: Oxford, 1997.

(38) Desiraju, G. R.; Steiner, T. *The Weak Hydrogen Bond in Structural Chemistry and Biology*; Oxford University Press: Oxford, 2001.

(39) Herzberg, G. *Molecular Spectra and Molecular Structure. I. Spectra of Diatomic Molecules*, 2nd ed.; Van Nostrand Reinhold Co.: New York, 1950.

(40) Cremer, D.; Kraka, E. *Angew. Chem.* **1984**, *23*, 627.

(41) Cremer, D.; Kraka, E. *Croat. Chem. Acta* **1984**, *57*, 1259.

(42) Cook, D. B.; Sordo, J. A.; Sordo, T. L. *Int. J. Quantum Chem.* **1993**, *48*, 375.

(43) Gonzalez, C.; Schlegel, H. B. *J. Chem. Phys.* **1989**, *90*, 2154.

(44) Gonzalez, C.; Schlegel, H. B. *J. Chem. Phys.* **1990**, *94*, 5523.

(45) Ruoff, R. S.; Klots, T. D.; Emilsson, T.; Gutowski, H. S. *J. Chem. Phys.* **1990**, *93*, 3142.

(46) *Chem. Rev.* **2000**, *100*, 3861−4264.

(47) See, for example, refs 14−15 and references therein.

(48) Andrews, A. M.; Hillig, K. W.; Kuczkowski, R. L.; Legon, A. C.; Howard, N. W. J. *J. Chem. Phys.* **1991**, *94*, 6947.

(49) Rayon, V. M.; Sordo, J. A. *Chem. Phys. Lett.* **2001**, *341*, 575.